Desalination and Water Treatment
www.deswater.com

doi: 10.5004/dwt.2018.22593

127 (2018) 83–89
September

Development of highly flux antifouling RO polyethersulfone membrane using compacted woven support

Marwa S. Shalaby[a,*], Vincenzo Naddeo[b], Laura Borea[b], Heba Abdallah[a], Ahmed M. Shaban[c], Tiziano Zarra[b], Vincenzo Belgiorno[b]

[a]*Chemical Engineering and Pilot Plant Department, Engineering Research Division, National Research Centre, 33 El Bohouth Street (Former El Tahrir Street), P.O. Box 12622, Dokki, Giza, Egypt, emails: marwashalaby14@gmail.com, marwashalaby_4@yahoo.com (M.S. Shalaby), heba_nasr94@yahoo.com, drhebaabdallah3@gmail.com (H. Abdallah)*

[b]*Sanitary Environmental Engineering Division (SEED), Department of Civil Engineering, University of Salerno, Via Giovanni Paolo II, 132, 84084 Fisciano, Salerno, Italy, Tel. +39 089969333; email: vnaddeo@unisa.it (V. Naddeo), Tel. +39 089969301; email: lborea@unisa.it (L. Borea), Tel. +39 089969335; email: tzarra@unisa.it (T. Zarra), Tel. +39 089969332; email: v.belgiorno@unisa.it (V. Belgiorno)*

[c]*Water Pollution Research Department, National Research Centre, 33 El Bohouth Street (Former El Tahrir Street), P.O. Box 12622, Dokki, Giza, Egypt, Tel. +202 33335494; Fax: +202 33370931; email: ashaban12311@gmail.com*

Received 31 January 2017; Accepted 5 June 2018

ABSTRACT

Over the next decades, many regions worldwide will likely face dramatic changes in the availability of water. Desalination of seawater appears as the perfect mean to ensure water supply. To this end, membrane filtration processes represent a promising technology since they can achieve high levels of purification and are simple technically, energy efficient, and typically scalable. However, membrane fouling, characterized by the deposition of solid material onto and into the membrane surface, is still the main problem of this treatment. In this work, novel highly flux antifouling membranes were prepared via phase inversion technique using polyethersulfone blending with a nanomaterials solution of sodium dodecyl sulfate, titanium dioxide (TiO_2), and triethanol amine, in *N*-methyl-2-pyrrolidone as a solvent. Three kinds of membranes were prepared: M1 without support, M2 with nonwoven support, and M3 with woven support. Desalination test was carried out using real samples from Mediterranean Sea. The scanning electron microscopy results prove that prepared membranes have dense top layer and small fingerlike structure in the middle, while the bottom layer is porous due to woven support. The prepared membrane using woven support exhibits excellent mechanical behavior. Furthermore, desalination test results indicate that salt rejection reached 96% at a high flux of 134.9 kg/m^2 h under operating pressure up to 40 bar and using the membrane with woven support.

Keywords: Antifouling; Polyethersulfone membranes; Desalination; Woven support

1. Introduction

Nowadays, development in membrane technology has raised great attention in improvement in membrane preparation process, environmental protection, health sector, desalination, and water treatment processes and new technologies for sustainable growth [1–4].

Most membrane fabrication processes depend on casting of polymeric solution on glass plate or nonwoven support using film applicator, and then the membrane formation step is carried out using coagulation bath which contains mostly water. Polyethersulfone (PES) membranes are mostly

---

* Corresponding author.

Presented at the 15th International Conference on Environmental Science and Technology (CEST-2017), 31 August–2 September 2017, Rhodes, Greece.

prepared without support or with nonwoven polyester support. The strength and mechanical properties of membranes [5] were greatly enhanced by using support materials which dominate in industrial scale applications [6]. Using support can limit shrinkage which provides stretching action on the nascent membrane during the coagulation stage, limiting its shrinkage [7,8]. Most special type of PES membrane support is nonwoven polyester. The merits of the prepared PES membrane supporting by nonwoven polyester is the improvement in mechanical properties, where the membranes can carry high pressure during operation [9,10]. Based on previous work on embedded nanomaterials to improve membrane performance like addition of titanium dioxide or carbon nanotubes or metal-organic compounds such as manganese acetylacetonate [11–13], these membranes have good performance but they are mostly without support so the mechanical properties are weak compared with supported membranes [14,15]. Forward osmosis membranes mostly were prepared using fabric support. Where, the prepared forward osmosis thin film composite (TFC) PES using woven support like a mesh provides improvement in the permeate flux without wrinkling formation [16].

Application of PES membrane on seawater desalination depends on the preparation of dense layer and/or TFC membrane by means of classical interfacial polymerization or blending techniques. However, recently doping TiO_2 nanotubes with PES in polymeric solution produces reverse osmosis (RO) membrane with high salt rejection (SR; 98%) and permeate flux (5.45 kg/m^2 h) [17]. TFC membrane is prepared using polysulfone or PES as a support, where polyamide layer is formed on the top surface of membrane using reaction between two monomers polyfunctional amine compounds in water and polyfunctional acid chloride in hydrocarbon solvent [18,19]. Asymmetric PES/Mn(acac)3 RO blend membranes were prepared by embedding metal-organic compound Mn(acac)3 in the polymer solution mixture that increased SR of seawater up to 99% [13].

The novelty of this work is the production of a novel blended membrane characterized by high mechanical and antifouling properties using compacted woven support as supporting material and by embedding titanium dioxide in the membrane matrix, respectively. On the other hand, compacted woven support leads to avoiding both membrane shrinkage and the defects associated with it.

The objective of this work is to get supported blend RO membrane with antifouling behavior due to innovative membrane preparation capable to carry high pressure for seawater desalination.

2. Materials and methods

2.1. Materials

PES (ultra son E6020P with MW = 58,000 g/mol) and Analytical grade *N*-methylpyrrolidone (NMP) as a solvent were purchased from BASF Company, Germany. Sodium dodecyl sulfate (SDS), triethanol amine (TEA), and Commercial TiO_2 anatase powder were obtained from Merck, Germany. All chemicals used in the experiments were of reagent grade. Woven support (satin yarn) was purchased from Egypt local market and nonwoven support (polyester) was purchased from Holykem company, China. Commercial TFC-RO membrane purchased from Aqua Chiara company, Egypt. Commercial NaCl was used in desalination experiments. Also, real seawater samples from Mediterranean Sea were obtained from Alexandria port in Egypt.

2.2. Fabrication of asymmetric RO PES membranes

The RO asymmetric PES membranes were fabricated by phase inversion induced by immersion precipitation method using casting solutions containing PES (20–25 wt.%), 6% nanomaterials solution containing 0.5% SDS, 1% TEA, and 1% TiO_2 in water. These chemicals were dissolved in NMP as solvent and stirred for 8 h and the polymer mixture solution was kept in refrigerator for 24 h to remove air bubbles.

Three kinds of membranes were fabricated: for the first, the polymeric solution (M1) was casted onto a clean glass plate with 100 μm thickness; for the second (M2), the polymeric solution was casted on a nonwoven support with 150 μm thickness; for the third one (M3), the polymeric solution was casted on woven support with 150 μm thickness. The casted membranes were immersed horizontally into distilled water at room temperature. Then, the membranes were stored in fresh distilled water for 24 h to complete phase separation.

2.3. Membrane characterization

2.3.1. Membrane morphology

Scanning electron microscopy (SEM) was used to study the morphology of prepared membranes, where the membranes samples of cross-sectional view were coated with gold to provide electrical conductivity. The cross-sectional snapshots of membrane were taken on a JEOL 5410 SEM and conducted at 10 kV.

2.3.2. Mechanical properties

Mechanical properties of the prepared membranes were investigated to determine the effect of support material variation on membrane strength. The tensile strength and membranes elongation were measured using mechanical testing system (INSTRON-5500R).

2.3.3. Membrane porosity and Brunauer–Emmett–Teller area

The inner surface of the prepared membranes was determined using the Brunauer–Emmett–Teller (BET) method. The analysis was conducted at the National Research Centre, Giza, Egypt. Samples of known weights of membrane were cut into long strips and placed in a glass column of the apparatus, dried and degassed by heating at 80°C for 3 h. The average area was determined using the BET single point. Porosity of prepared membranes was also determined from this test.

2.4. Membrane performance measurements

The experiments were carried out on the laboratory desalination unit as shown in Fig. 1. This system contains

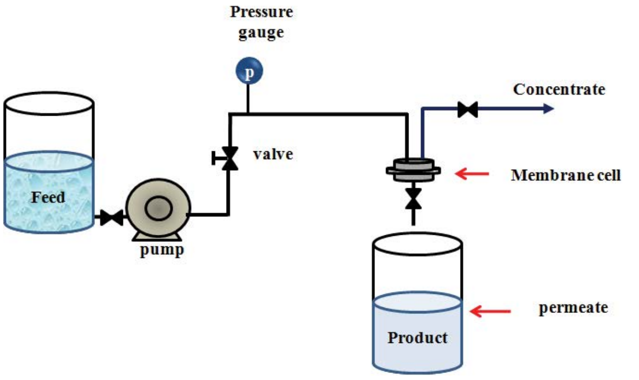

Fig. 1. Schematic drawing of laboratory desalination testing unit.

flat sheet membrane module of three openings for feeding, concentrate, and permeate.

The feed was continuously fed to the membrane module from a closed feeding tank (50 L) using a high-pressure pump. The product was collected from downstream of the membrane module. Different prepared membranes were located in stainless steel plate module of 10 cm in diameter. In all experiments, Mediterranean Sea samples characterized by concentration of total dissolved salts (TDS) equal to 35,800 ppm were continuously fed to the membrane module at 50 bar pressure and temperature of 25°C. Table 1 illustrates the characterization of seawater sample. Also different synthetic solutions (20,000, 35,000 and 40,000 ppm), using commercial NaCl, were prepared and tested on the same kinds of membranes.

For this system, the water flux J_w (kg/m^2 h) is given by the following equation:

$$J_w = \frac{V \cdot \rho}{A \cdot t} \tag{1}$$

where V is the volume of the pure water permeate (m^3), A is the effective area of the membrane (m^2), ρ is the water density (kg/m^3), and t is the permeation time (h).

The TDS of the produced water was measured using a conductivity meter called Adwa (AD 310), EC/temp meter made in Romania. It has an electrical conductivity range from 19.99 μS/cm to 199.9 mS/cm, where 1 mS/cm is equal approximately to 670 ppm.

Table 1
Sea water sample characterization

Parameters	Result
Total dissolved salts (mg/L) (ppm)	35,800
pH	7.5
Total hardness (mg/L)	5,760
Calcium hardness (mg/L)	1,760
Magnesium hardness (mg/L)	4,000
Sodium (mg/L)	16,040
Alkalinity as bicarbonates (mg/L)	14,000
Hydroxides (mg/L)	0
Carbonates (mg/L)	0.004

In addition, the SR% was conducted in triplicates for each membrane and the average result was calculated using the following equation:

$$\text{SR\%} = \frac{C_f - C_p}{C_f} \times 100 \tag{2}$$

where C_f and C_p are concentrations (mg/L) at feed bulk and permeate, respectively.

2.5. Membrane fouling testing

Experiments were carried out using the same desalination laboratory unit on whey solution to expose the membranes to extreme level of fouling and on seawater. Firstly, the distilled water was permeated through membranes for 3 h [17] and the permeate flux J_{w1} was measured. Secondly, the whey solution in pH = 7.0 ± 0.1 was permeated through membranes for 3 h. The permeate flux J_p (kg/m^2 h) was measured based on the amount of produced water permeated from the membranes at 30 bar for 3 h. The fouled membranes were washed with distilled water for 30 min after removing the whey solution. Finally, distilled water was passed though membranes again for 3 h and the permeate flux was measured J_{w2} (kg/m^2 h). The same sequence was repeated using sea water. The flux recovery ratio (FRR) was calculated as follows:

$$\text{FRR\%} = \frac{J_{w2}}{J_{w1}} \times 100 \tag{3}$$

The total fouling ratio (R_t) was calculated as following:

$$R_t\% = \left(1 - \frac{J_p}{J_{w1}}\right) \times 100 \tag{4}$$

where R_t is the degree of total flux loss caused by total fouling. Reversible fouling ratio (R_r) and irreversible fouling ratio (R_{ir}) can be calculated by following equations, respectively [20–22]:

$$R_r\% = \left(\frac{J_{w2} - J_p}{J_{w1}}\right) \times 100 \tag{5}$$

$$R_{\text{ir}}\% = \left(\frac{J_{w1} - J_{w2}}{J_{w1}}\right) \times 100 \tag{6}$$

Generally, R_t is the sum of R_r and R_{ir}.

3. Results and discussion

3.1. Characterization of asymmetric PES RO

3.1.1. Membrane morphology

Fig. 2 shows cross-sectional SEM image of prepared membrane without support (M1). The membrane has asymmetric structure with top dense layer, a porous sublayer, and large macropores at the bottom.

Fig. 3 illustrates cross section of the fabricated membrane using nonwoven support (M2). The image indicates highly dense top layer, with narrow wall of fingerlike structure in

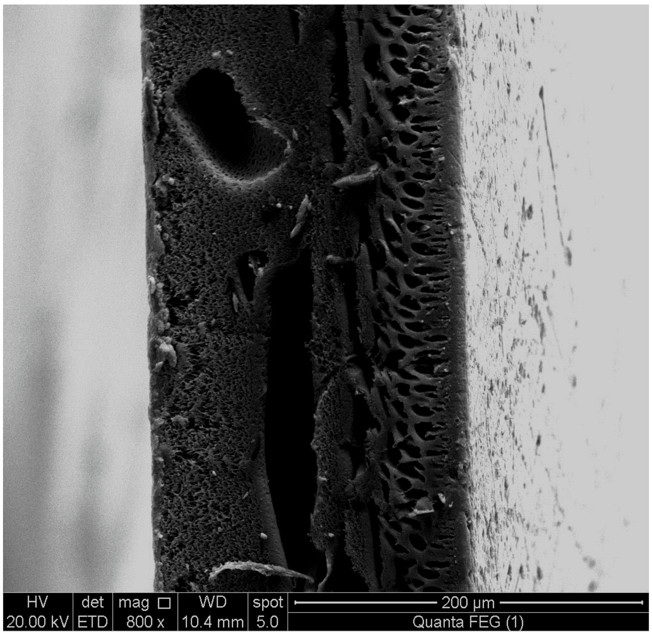

Fig. 2. The cross-sectiontal SEM images of prepared membrane (M1) without support.

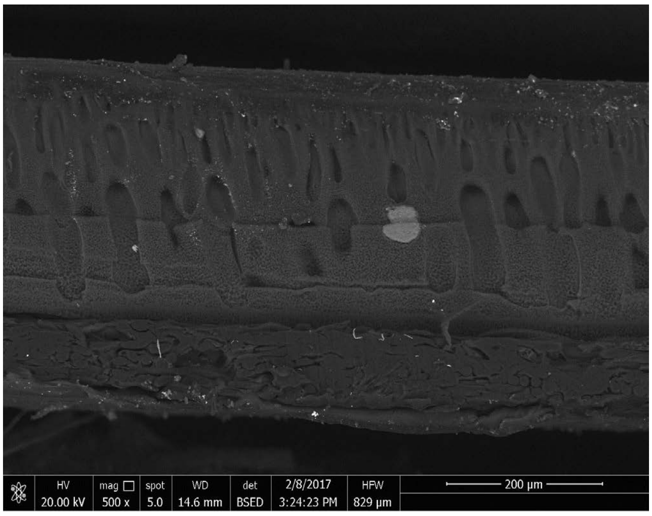

Fig. 3. The cross-sectiontal SEM images of prepared membrane (M2) with nonwoven support.

the middle due to addition of nanoparticles of SDS and titanium dioxide in the polymeric solution. The bottom layer has compacted structure of nonwoven support.

Fig. 4 illustrates cross section of the fabricated membrane using woven support (M3). The snapshot indicates highly dense top layer, with small length of fingerlike structure in the middle due to impregnation of the woven support fabric part of the polymeric solution. The bottom layer has porous structure according to the woven support pores. Using nanoparticles solution of SDS and titanium dioxide in the polymeric solution leads to denser structure in top layer due to delay in phase separation during membrane formation as increasing in the polymeric solution viscosity [11].

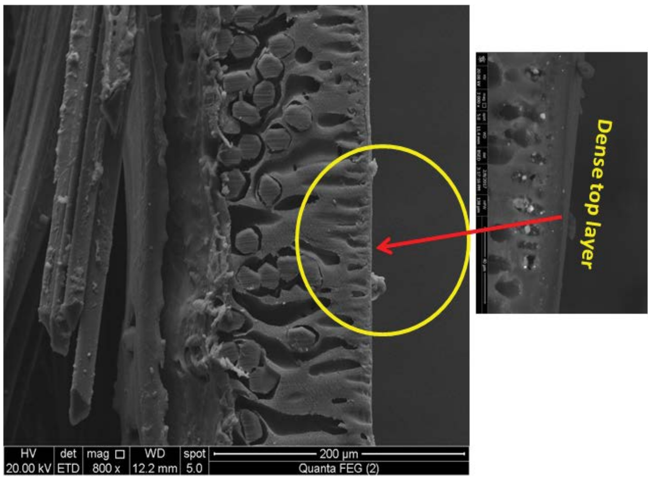

Fig. 4. The cross-sectiontal SEM images of prepared membrane (M3) with woven support.

3.1.2. Mechanical properties

The tensile strength and elongation of the blend membrane was obtained using mechanical testing system. Fig. 5 shows the relation between tensile strength, elongation, and the support type. As can be seen in Fig. 5, the maximum tensile strength and elongation for M3 were equal to 152 kg/m^2 and 36.6%, respectively. This can be attributed to using woven support, which enhances tensile strength and elongation due to properties of woven fabric along the grain and closer to the weave gives stronger and firmer fabric.

3.1.3. Membrane porosity and BET area

For all the prepared PES membranes with different supports, the pore size distribution became narrower around the mean pore diameters. The total pore volume and the mean pore diameter are listed in Table 2. It can be found that the pore size of the PES membranes was in nanosize due to the

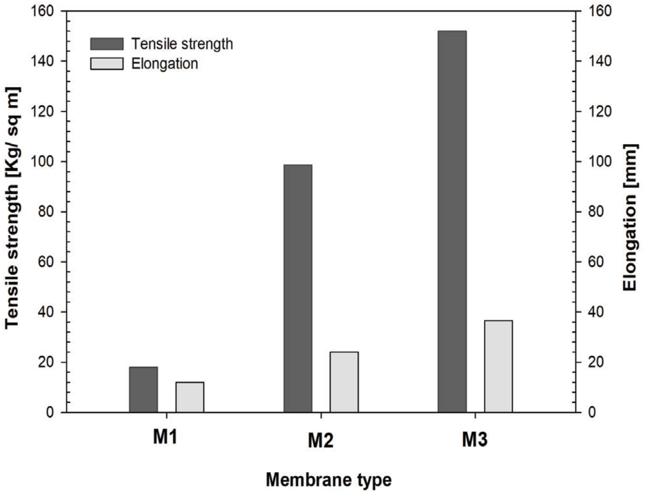

Fig. 5. Mechanical properties of prepared membranes, M1: membrane without support, M2: membrane with nonwoven support, and M3: membrane with woven support.

Table 2
Measurement of BET area and pores characterization

Membrane type	BET area (m^2/g)	Total pore volume (cm^3/g)	Mean pore diameter (nm)	Porosity
M1	6.7	1.092E-2	6.5	35.7
M2	6.75	1.0925E-2	6.47	35.6
M3	7.8E-2	1.72E-2	8.8	40.9

use of titanium dioxide and SDS, which was in agreement with the analysis of membrane morphology. M3 provides porosity of 40.9%, which is the highest one and highest BET area according to using woven support showing better pore distribution all over membrane surface.

M1, the one casted without support, showed a lower porosity when compared with M3. The pores in the unsupported membranes are much smaller than the supported one as a result of shrinkage of unsupported membrane [14]. For M2, it was noticed that the viscous polymeric solution penetrates the voids of support and sufficient penetration into nonwoven support is necessary to allow a good integration of the PES matrix [14]. While M3, the membrane with woven support, had a compacted backing, which block polymer solution limiting surface wrinkle, defected problems, and prevented polymer penetration through voids, leading to the formation of three layers: highly porous bottom layer, finger intermediate layer, and dense top layer [16].

3.2. Membrane performance measurements

Average water permeate flux and average SR% of prepared membranes with different supports were studied using laboratory desalination system unit. The effects of support on water flux and SR% of prepared membranes using different synthetic salt water concentrations (20,000, 35,000, and 45,000 ppm) together with real seawater of salinity 35,800 ppm are shown in Figs. 6 and 7, respectively. The average flux reached to maximum using M3 with woven support, while, the SR in all feed concentration is close to each other. Using M3 membrane with the seawater samples, the SR reached to 96% at a high flux of 134.9 kg/m^2 h under operating pressure up to 40 bar.

The results indicated improvement in rejection percentage for the separation of all salt concentration using compacted woven support.

The highest permeate flux was given with M3 for woven support due to small fingerlike structure shown in membrane SEM, which improves membrane porosity to reach 40.9%. While, for nanomaterials present on the polymeric solution, it was clearly responsible for the dense selective top layer of the membrane.

SR depends on the selective layer of membrane, which must be a dense layer for RO desalination. On the other hand, the prepared polymer solution is the same for all membranes, while the difference is the support material used in membrane casting. So, the support materials show here a high influence over pore size distribution that can increase the rejection percentage and permeate flux depending on porosity of such membranes. However, the selective dense layer has the same structure for all membranes, so the rejection percentages for all membranes are close to each other [11,12].

3.3. Membrane fouling testing

The anti-biofouling and fouling performance of the prepared membrane, M3 and TFC-RO as a commercial membrane, were tested by measuring of water flux recovery after fouling by whey solution and seawater, respectively.

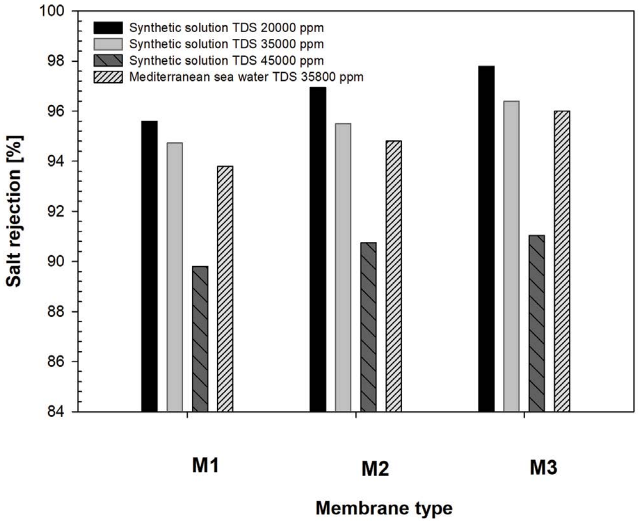

Fig. 6. Effect of support on salt rejection of prepared membranes, M1: membrane without support, M2: membrane with nonwoven support, and M3: membrane with woven support.

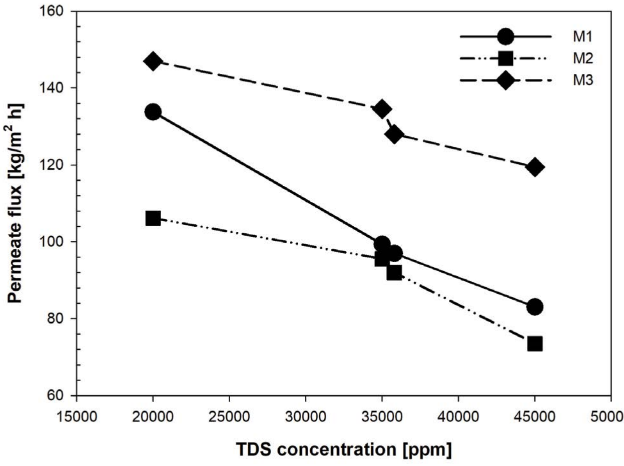

Fig. 7. Effect of support on salt permeate flux of prepared membranes, M1: membrane without support, M2: membrane with nonwoven support, and M3: membrane with woven support.

M3 was selected according to the best flux and rejection depending on the support effect on the performance of the membrane. However, the polymeric solution was the same for all prepared membranes and the performance of membranes are changed depending on support material, while the fouling depends on the membrane surface not the bottom of the membrane, so the dense top layer effects on the fouling test, not the support.

The fouling can occur due to different parameters such as interactions between molecules and membrane surface, polymer chemistry, pH of solution, and membrane structure [11]. Fig. 8 illustrates the biofouling test, where the pure water fluxes before and after whey separation were measured and permeate flux solution from whey separation was also measured. After that, the FRR and resistance parameters were calculated to assess the anti-biofouling properties.

Fig. 8 indicates that the permeate flux of membrane (M3) decreases after using whey solution due to several factors such as high fouling of membrane and concentration polarization. The fouling of membrane may be attributed to adsorption or deposition of protein molecules on the membrane surface. Small pores on the top membrane surface being clogged will play an important role for flux decline and carry a good interpretation for membrane fouling. FRR was calculated for M3 and found to be 78.9% compared with TFC-RO membrane, which was only 69.2%. The higher FRR shows good antifouling property for prepared M3 compared with the commercial membrane. Reversible resistance R_r was 37.9% for M3 and 61.5% for TFC-RO, the adsorption of protein on the membrane surface causes reversible fouling, which was easily removed by backwash. The results indicate that high reversible resistance for TFC-RO was shown when compared with M3, which is an indication to formation of protein cake layer on membrane surface. Irreversible fouling was present due to clogging of pores with protein molecules, where R_{ir} was 21.05% for M3 and increased to reach 30.8% for TFC-RO. R_t was 58.9% for M3 and 92.3% for TFC-RO membrane. The results indicate that M3 can be considered to be effective antifouling membrane compared with TFC-RO membrane, regarding that biofouling can be easily removed by back and surface washing of membrane M3, while high irreversible resistance of TFC-RO is an indication of pore clogging by protein molecules [12].

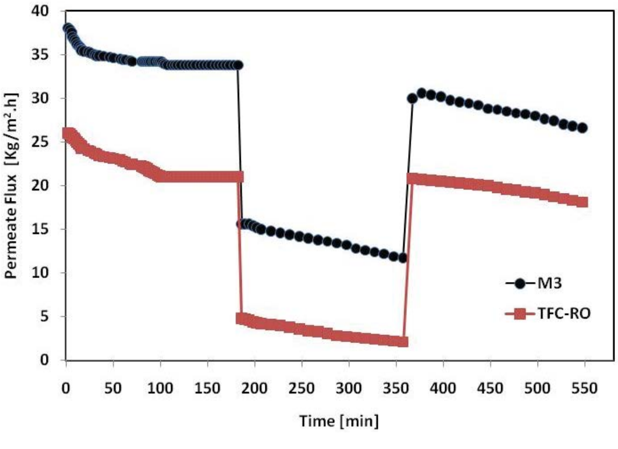

Fig. 8. Permeate flux verses time for prepared membrane supported by woven support (M3) compared with commercial TFC-RO membrane during biofouling test.

On the other hand, antifouling test using seawater was studied as the same sequence of whey solution on M3 and commercial TFC-RO membrane. Fig. 9 illustrates that the permeate flux of M3 decreases after using seawater due to concentration polarization and diffusion of salts through the membrane pores, which causes fouling. Meanwhile, FRR was calculated for M3 showing an enhancement of antifouling behavior to reach 94.5% when compared with TFC-RO, which was about 90%. The total fouling ratio (R_t) was calculated and found to be 59.74% for M3 and 61.5% for TFC-RO. The reversible fouling ratio (R_r) was found to be 54.2% and 53.46% for M3 and TFC-RO respectively; while for irreversible fouling ratio (R_{ir}) was 5.53% for M3 and 10% for TFC-RO, showing the adverse effect of reversible fouling for both membranes. M3 shows advantage over commercial one that it has a lower irreversible resistance interpreted in its low tendency to pores clogging. This kind of foulants can be easily removed by surface membrane cleaning, while low values of irreversible fouling ratio indicate that the presence of nanotitanium dioxide with SDS blended with PES increases membrane hydrophilicity which in turn decreases its pores size. The improvement of membranes hydrophilicity leads to enhancement of water flux due to attraction of molecules of water into the membrane surface and matrix of membrane to pass easily through it [23]. Also, hydrophilic surface reduces the adsorption of any contamination in the feeding water to the membrane surface [24]. Moreover, blending of nanomaterials with polymer in membrane preparation provides smooth surface, which also reduces fouling [25]. Also, titanium oxide and its catalytic activity, which reduces membrane fouling, can be attributed to mineralization. Its effect means that organic molecules or microorganisms in water can be destroyed by oxidation, where an electron–hole forms hydroxyl radicals which are more powerful oxidizing agents compared with chlorine or ozone (O_3^+) [26]. The membrane also acquires a property of being photocatalytic; when a group of oxygen vacancies is produced on the surface, the water molecules can occupy the empty sites and lead to an increase in the hydrophilicity of the membrane surface [13]. Also, the produced radicals on the surface can prevent the deposition of proteins and salts which is the reason of the fouling.

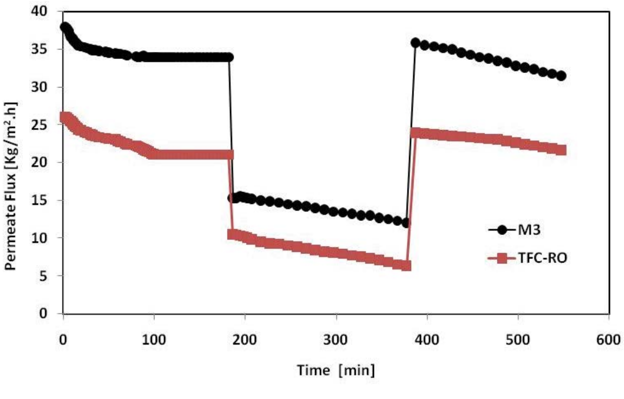

Fig. 9. Permeate flux verses time for prepared membrane supported by woven (M3) compared with commercial TFC-RO membrane during fouling test using seawater.

The irreversible fouling for M3 is higher than reversible fouling for whey solution; that may be attributed to the dense top layer, which has too small pores easily clogged with protein molecules. Knowing that, protein size has large molecules size compared with the salt molecules in seawater. However, seawater can be easily removed by back wash; but for protein, it shows some difficulties depending on adsorption and desorption on the membrane surface [12].

4. Conclusion

The asymmetric antifouling membranes of PES blending with a nanomaterials solution of SDS, titanium dioxide (TiO_2), and TEA, in *N*-methyl-2-pyrrolidone (NMP) were successfully fabricated by phase inversion method without and with using woven and non woven supporting fabric. Membrane using woven support exhibits highest mechanical properties and provides excellent results for all salt concentrations. Antifouling testing on membrane using woven support was studied using whey solution and seawater. The SR reached to 96% with high flux of 134.9 kg/m^2 h under operating pressure up to 40 bar using samples from Mediterranean Sea and membrane with woven support. Membrane with woven support provides superior fouling resistance where FRR was 70.53% at using whey and 94.5% using seawater.

Acknowledgments

The research activities were partially funded by FARB projects of the University of Salerno and the project no. IN17GR09 funded by Italian Ministry of Foreign Affairs and International Cooperation and Indian Ministry of Science and Technology. The research activities were also partially funded by National Research Centre (NRC) for the STDF funded Italian Egyptian project no. 25920 linked to the international project no. EG16MO01 of the Italian Ministry of Foreign Affairs. The authors gratefully thank colleagues from central laboratory and flat sheet membrane group in NRC for the cooperation and the precious help given during the research activity.

References

[1] V.V. Goncharuk, A.A. Kavitskaya, M.D. Skil'skaya, Nanofiltration in drinking water supply, J. Water Chem. Technol., 33 (2011) 37–54.

[2] M.R. Sohrabi, S.S. Madaeni, M. Khosravi, A.M. Ghaedi, Concentration of licorice aqueous solutions using nanofiltration and reverse osmosis membranes, Sep. Purif. Technol., 75 (2010) 121–126.

[3] M.N. Abu Seman, M. Khayet, N. Hilal, Development of antifouling properties and performance of nanofiltration membranes modified by interfacial polymerization, Desalination, 273 (2011) 36–47.

[4] L. Borea, V. Naddeo, M.S. Shalaby, T. Zarra, V. Belgiorno, H. Abdallah, A.M. Shaban, Wastewater treatment by membrane ultrafiltration enhanced with ultrasound: effect of membrane flux and ultrasonic frequency, Ultrasonics, 83 (2018) 42–47.

[5] P. Aerts, I. Genné, R. Leysen, P.A. Jacobs, I.F.J. Vankelecom, The role of the nature of the casting substrate on the properties of membranes prepared via immersion precipitation, J. Membr. Sci., 283 (2006) 320–327.

[6] D. Hou, H. Fan, Q. Jiang, J. Wang, X. Zhang, Preparation and characterization of PVDF flat-sheet membranes for direct contact membrane distillation, Sep. Purif. Technol, 135 (2014) 211–222.

[7] A. Bottino, G. Capannelli, A. Comite, M. Oliveri, Development of novel membranes with controlled porosity from fluorinated polymer, Filtration, 4 (2004) 130–135.

[8] G. Kang, Y. Cao, Application and modification of poly(vinylidene fluoride) (PVDF) membranes – a review, J. Membr. Sci., 463 (2014) 145–165.

[9] C. Feng, B. Shi, G. Li, Y. Wu, Preliminary research on microporous membrane from F2.4 for membrane distillation, Sep. Purif. Technol., 39 (2004) 221–228.

[10] H. Fan, Y. Peng, Z. Li, P. Chen, Q. Jiang, S. Wang, Preparation and characterization of hydrophobic PVDF membranes by vapor-induced phase separation and application in vacuum membrane distillation, J. Polym. Res., 20 (2013) 1–15.

[11] H. Abdallah, A.F. Moustafa, A. AlAnezi, H.E.M. El-Sayed, Performance of a newly developed titanium oxide nanotubes/polyethersulfone blend membrane for water desalination using vacuum membrane distillation, Desalination, 346 (2014) 30–36.

[12] M. Shaban, H. AbdAllah, L. Said, H.S. Hamdy, A. Abdel khalek, Titanium dioxide nanotubes embedded mixed matrix PES membranes characterization and membrane performance, Chem. Eng. Res. Des., 95 (2015) 307–316.

[13] H. Abdallah, M.S. Shalaby, A.M.H. Shaban, Performance and characterization for blend membrane of PES with manganese(III) acetylacetonate as metalorganic nanoparticles, Int. J. Chem. Eng., 2015 (2015) 1–9.

[14] M.R. Bilad, E. Guillen-Burrieza, M.O. Mavukkandy, F.A. AlMarzooqi, H.A. Arafat, Shrinkage, defect and membrane distillation performance of composite PVDF membranes, Desalination, 376 (2015) 62–72.

[15] Y. Yang, D. Rana, T. Matsuura, S. Zheng, C.Q. Lan, Criteria for the selection of a support material to fabricate coated membranes for a life support device, RSC Adv., 4 (2014) 38711–38717.

[16] S. Sahebi, S. Phuntsho, L. Tijing, G. Hanb, D.S. Han, A. Abdel-Wahab, H. KyongShon, Thin-film composite membrane on a compacted woven backing fabric for pressure assisted osmosis, Desalination, 406 (2017) 98–108.

[17] M. Shaban, H. Abdallah, L. Said, H.S. Hamdy, A. Abdel khalek, Fabrication of PES/TiO_2 nanotubes reverse osmosis (RO) membranes, J. Chim. Acta, 2 (2013) 59–61.

[18] K.G. Asim, E.M.V. Hoek, Impacts of support membrane structure and chemistry on polyamide–polysulfone interfacial composite membranes, J. Membr. Sci., 336 (2009) 140–148.

[19] E. Elzanati, H. Abdallah, Interfacially synthesized thin film composite nanofiltration flat sheet membrane by flow through process, Eur. J. Sci. Res., 127 (2014) 284–297.

[20] J. Peng, Y. Su, Q. Shi, W. Chen, Z. Jiang, Protein fouling resistant membrane prepared by amphiphilic pegylated polyethersulfone, Bioresour. Technol., 102 (2011) 2289–2295.

[21] S. Kang, A. Asatekin, M. Elimelech, A.M. Mayes, Protein antifouling mechanisms of PAN UF membranes incorporating PAN-g-PEO additive, J. Membr. Sci., 296 (2007) 42–50.

[22] S.S. Madaeni, N. Ghaemi, Characterization of self-cleaning RO membranes coated with TiO_2 particles under UV irradiation, J. Membr. Sci., 303 (2007) 221–233.

[23] J. Zhang, Z. Xu, W. Mai, C. Min, B. Zhou, M. Shan, Y. Li, C. Yang, Z. Wang, X. Qian, Improved hydrophilicity, permeability, antifouling and mechanical performance of PVDF composite ultrafiltration membranes tailored by oxidized low dimensional carbon nanomaterials, J. Mater. Chem. A, 1 (2013) 3101–3111.

[24] T. Wu, B. Zhou, T. Zhu, J. Shi, Z. Xu, C. Hu, J. Wang, Facile and low-cost approach towards a PVDF ultrafiltration membrane with enhanced hydrophilicity and antifouling performance via graphene oxide/water-bath coagulation, RSC Adv., 5 (2015) 7880–7889.

[25] Z. Xu, J. Zhang, M. Shan, Y. Li, B. Li, J. Niu, B. Zhou, X. Qian, Organosilane-functionalized graphene oxide for enhanced antifouling and mechanical properties of polyvinylidene fluoride ultrafiltration membranes, J. Membr. Sci., 458 (2014) 1–13.

[26] Z. Xu, T. Wu, J. Shi, K. Teng, W. Wang, M. Ma, J. Li, X. Qian, C. Li, J. Fan, Photocatalytic antifouling PVDF ultrafiltration membranes based on synergy of graphene oxide and TiO_2 for water treatment, J. Membr. Sci., 520 (2016) 281–293.